J|A|C|S
ARTICLES
Published on Web 08/12/2006

Remarkable Aspects of Unsaturation in Trinuclear Metal Carbonyl Clusters: The Triiron Species $Fe_3(CO)_n$ (n = 12, 11, 10, 9)

Hongyan Wang,*[,†,‡] Yaoming Xie,[‡] R. Bruce King,*[,‡] and Henry F. Schaefer, III[‡]

Contribution from the Atomic and Molecular Physics Institute, Sichuan University, Chengdu 610065, P.R. China, and Department of Chemistry and Center for Computational Chemistry, University of Georgia, Athens, Georgia 30602

Received August 11, 2005; E-mail: wanghyxx@scu.edu.cn; rbking@chem.uga.edu

Abstract: The trinuclear iron carbonyls $Fe_3(CO)_n$ (n = 12, 11, 10, 9) have been studied by density functional theory using the B3LYP and BP86 functionals. The experimentally known C_{2v} isomer of $Fe_3(CO)_{12}$, namely $Fe_3(CO)_{10}(\mu\text{-}CO)_2$, is found to be the global minimum below the unbridged D_{3h} isomer analogous to the known structures for $Ru_3(CO)_{12}$ and $Os_3(CO)_{12}$. The lowest-energy isomer found for $Fe_3(CO)_{11}$ is $Fe_3(CO)_9(\mu_3\text{-}CO)_2$ with iron−iron distances in the Fe_3 triangle, suggesting the one double bond (2.460 Å by B3LYP and 2.450 Å by BP86) and two single bonds (2.623 Å by B3LYP and 2.604 Å by BP86) required to give each Fe atom the favored 18-electron configuration. Two different higher-energy dibridged structures $Fe_3(CO)_9(\mu_2\text{-}CO)_2$ are also found for $Fe_3(CO)_{11}$. The lowest-energy isomer found for $Fe_3(CO)_{10}$ is $Fe_3(CO)_9(\mu_3\text{-}CO)$ with equivalent iron−iron distances in the Fe_3 ring (2.47 Å by B3LYP or BP86). The lowest-energy isomer found for $Fe_3(CO)_9$ is $Fe_3(CO)_6(\mu\text{-}CO)_3$ with distances in the Fe_3 triangle possibly suggesting one single bond (2.618 Å by B3LYP and 2.601 Å by BP86), one weak double bond (2.491 Å by B3LYP and 2.473 Å by BP86), and one weak triple bond (2.368 Å by B3LYP and 2.343 Å by BP86). A higher-lying isomer of $Fe_3(CO)_9$, i.e., $Fe_3(CO)_8(\mu\text{-}CO)$, at ∼21 kcal/mol above the global minimum, has iron−iron distances strongly suggesting two single bonds (2.6 to 2.7 Å) and one quadruple bond (2.068 Å by B3LYP and 2.103 Å by BP86). Wiberg Bond Indices are also helpful in evaluating the iron−iron bond orders.

1. Introduction

Trinuclear metal carbonyl clusters have been known since the isolation of $Fe_3(CO)_{12}$ by Dewar and Jones in 1907.[1] However, elucidation of the correct structure of $Fe_3(CO)_{12}$ followed a tortuous route.[2] The trimeric nature of $Fe_3(CO)_{12}$ was first established by Hieber and Becker[3,4] only in 1930 using cryoscopy in $Fe(CO)_5$. The correct isosceles triangular structure of $Fe_3(CO)_{12}$ with two bridging CO groups, i.e., $Fe_3(CO)_{10}(\mu\text{-}CO)_2$ (Figure 1b: M = Fe), was first determined by X-ray diffraction in 1966 by Wei and Dahl after considerable disorder problems.[5] More accurate geometrical parameters for $Fe_3(CO)_{12}$ were subsequently determined by Cotton and Troup[6] and later by Braga, Grepioni, Farrugia, Johnson.[7] The analogous triangular ruthenium and osmium carbonyls $M_3(CO)_{12}$ (M = Ru, Os) were synthesized later. After original misidentification as $M_2(CO)_9$, their correct structures were found by X-ray diffraction[8−10] to have similar metal triangles but without bridging carbonyl groups (Figure 1a: M = Ru, Os).

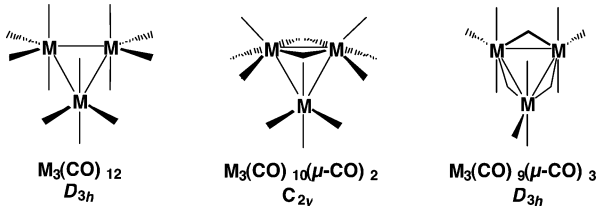

Figure 1. Structures of $M_3(CO)_{12}$ isomers: (a) $M_3(CO)_{12}$ with no bridging CO groups (D_{3h}); (b) $M_3(CO)_{10}(\mu\text{-}CO)_2$ with two bridging CO groups (C_{2v}); (c) $M_3(CO)_9(\mu\text{-}CO)_3$ with three bridging CO groups (D_{3h}). For clarity the CO groups are omitted.

The chemical bonding in the M_3 triangles of $M_3(CO)_{12}$ (M = Fe, Ru, Os), regardless of the number of bridging CO groups, is generally assumed to consist of three M−M two-center two-electron (2c-2e) single σ-bonds along the edges of the M_3 triangles (Figure 2a). Such a simple edge-localized bonding model gives each of the metal atoms the favored 18-electron rare gas configuration.[11−13] Since the three $M(CO)_4$ fragments comprising the structures of $M_3(CO)_{12}$ are isolobal to CH_2 fragments in hydrocarbon chemistry, the trinuclear metal carbonyls $M_3(CO)_{12}$ may be considered through isolobality to

† Sichuan University.
‡ University of Georgia.

(1) Dewar, J.; Jones, H. O. *Proc. R. Soc.* **1907**, *79A*, 66.
(2) Desiderato, R.; Dobson, G. R. *J. Chem. Educ.* **1982**, *59*, 752.
(3) Hieber, W.; Becker, E. *Chem. Ber.* **1930**, *63*, 1405.
(4) Hieber, W. *Z. Anorg. Allg. Chem.* **1932**, *203*, 165.
(5) Wei, C. H.; Dahl, L. F. *J. Am. Chem. Soc.* **1966**, *88*, 1821.
(6) Cotton, F. A.; Troup, J. M. *J. Am. Chem. Soc.* **1974**, *96*, 4155.
(7) Braga, D.; Grepioni, F.; Farrugia, L. J.; Johnson, B. F. G. *J. Chem. Soc., Dalton Trans.* **1994**, 2911.
(8) Mason, R.; Rae, A. I. M. *J. Chem. Soc. A* **1968**, 778.
(9) Churchill, M. R.; DeBoer, B. G. *Inorg. Chem.* **1977**, *16*, 878.
(10) Corey, E. R.; Dahl, L. F. *J. Am. Chem. Soc.* **1961**, *83*, 2203.
(11) Langmuir, I. *Science* **1921**, *54*, 59.
(12) Sidgwick, N. V.; Bailey, R. W. *Proc. R. Soc. London* **1934**, *A144*, 521.
(13) Pyykkö, P. *J. Organomet. Chem.* **2006**, submitted.

10.1021/ja055223+ CCC: $33.50

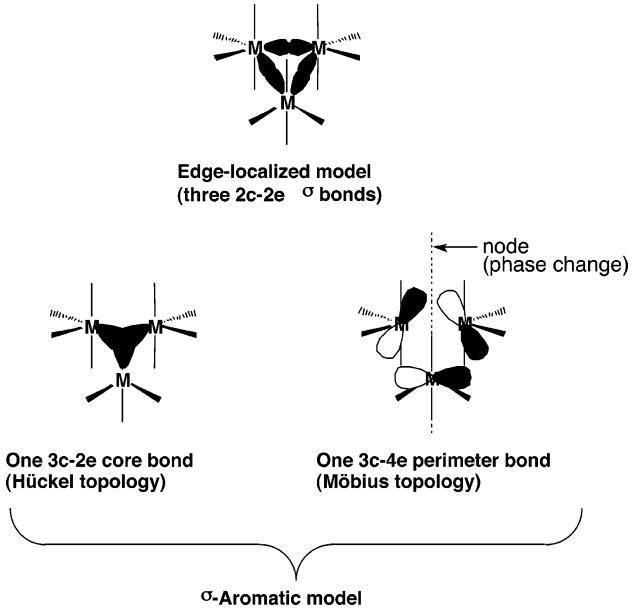

Figure 2. (a) Edge-localized bonding model for $M_3(CO)_{12}$ showing the three 2c-2e σ bonds: (b) σ-Aromatic model for $M_3(CO)_{12}$ showing the 3c-2e core bond with Hückel topology and the 3c-4e perimeter bond with Möbius topology.

be metal carbonyl analogues of cyclopropane. An alternative bonding model for cyclopropane and for the triangular metal carbonyls is the so-called σ-aromaticity model,[14−19] which accounts for the stability of triangular clusters relative to that of square clusters despite the higher angular strain in triangles. In metal carbonyl chemistry the effect of σ-aromaticity is demonstrated by the much larger thermal stability of triangular $Os_3(CO)_{12}$ relative to that of square $Os_4(CO)_{16}$.[20] The σ-aromaticity model for bonding in triangular clusters replaces the three 2c-2e bonds in the edge-localized bonding model (Figure 2a) with one 3c-2e core bond having the normal Hückel topology and one 3c-4e perimeter bond having Möbius topology. The latter corresponds to a single phase change of the participating p-type orbitals (Figure 2b). Note that both bonding models use six orbitals and six electrons for the skeletal bonding in a triangular cluster and thus are indistinguishable by simple electron counting.

This paper uses density functional theory (DFT) methods to examine the relative energies of three types of structures for $Fe_3(CO)_{12}$, namely structures without bridging CO groups as well as those with two and three bridging CO groups (Figure 1). In addition, the unsaturated species $Fe_3(CO)_n$ (n = 11, 10, and 9) are similarly examined in order to determine whether their most favorable isomers use metal−metal multiple bonding, four- or six-electron donor CO groups, and/or metal electronic configurations less than 18 electrons to accommodate their unsaturation. All three of these possibilities have been encountered in our previous work on unsaturated binuclear metal carbonyls of the first-row transition metals from chromium to copper.[21−24] Finally this paper discusses the radical anion $Fe_3(CO)_{11}^{\bullet-}$, which has been characterized structurally by X-ray diffraction as its tetraphenylphosphonium salt.[25]

The first DFT investigation of the electronic structure of $Fe_3(CO)_{12}$ was carried out by Rosa and Baerends.[26] Subsequently, Jang and collaborators[27] studied the electronic structure and predicted the vibrational frequencies for $Fe_3(CO)_{12}$ with hybrid Hartree−Fock/DFT methods. In these studies the dibridged C_{2v} structure of $Fe_3(CO)_{12}$ (Figure 1b: M = Fe) was constructed by replacing one of the bridging CO groups in the known tribridged structure of $Fe_2(CO)_9$ (i.e., $Fe_2(CO)_6(\mu\text{-}CO)_3$) with an $Fe(CO)_4$ group. However, the structural parameters of $Fe_3(CO)_{12}$ from X-ray and ^{13}C NMR spectroscopy show that the unbridged D_{3h} structure (Figure 1a: M = Fe) lies only about 10 kcal/mol above the C_{2v} dibridged structure (Figure 1b: M = Fe).[9,28] Recently the bonding in the D_{3h} and C_{2v} isomers of $Fe_3(CO)_{12}$ has been studied using two complementary topological approaches, namely the atoms-in-molecules (AIM) theory and the analysis of the electron localization function (ELF).[29] Both methods indicate that the stabilization of the dibridged (C_{2v}) isomer of $Fe_3(CO)_{12}$ arises mainly from the presence of the two bridging CO groups, which take advantage of a rather large electron transfer from the iron atoms.

The unsaturated neutral species $Fe_3(CO)_{11}$ and $Fe_3(CO)_{10}$ apparently have not been studied either experimentally or theoretically. However, both the radical anion[25] $Fe_3(CO)_{11}^{\bullet-}$ and the dianion[30] $Fe_3(CO)_{11}^{2-}$ have been characterized structurally by X-ray diffraction as salts of suitable large countercations. The more highly unsaturated $Fe_3(CO)_9$ is also unknown experimentally but has been studied by extended Hückel molecular orbital (EHMO) theory.[31]

2. Theoretical Methods

Basis sets have been chosen to provide continuity with a body of existing research on organometallic compounds. Fortunately, DFT methods are far less sensitive to basis set than the higher-level methods such as coupled cluster theory. In this work the double-ζ plus polarization (DZP) basis sets used for carbon and oxygen add one set of pure spherical harmonic d functions with orbital exponents $\alpha_d(C) = 0.75$ and $\alpha_d(O) = 0.85$ to the Huzinaga−Dunning standard contracted DZ sets and are designated (9s5p1d/4s2p1d).[32,33] For Fe, in our loosely contracted DZP basis set, the Wachters' primitive set is used but is augmented by two sets of p functions and one set of d functions, contracted following Hood et al., and designated (14s11p6d/10s8p3d).[34,35] For $Fe_3(CO)_9$, $Fe_3(CO)_{10}$, $Fe_3(CO)_{11}$, and $Fe_3(CO)_{12}$ there are 417, 447, 477, and 507 contracted Gaussian functions, respectively.

(14) Dewar, M. J. S.; Pettit, R. *J. Chem. Soc.* **1954**, 1625.
(15) Dewar, M. J. S. *Bull. Soc. Chim. Belg.* **1979**, *88*, 957.
(16) Dewar, M. J. S.; McKee, M. L. *Pure Appl. Chem.* **1980**, *52*, 1431.
(17) Dewar, M. J. S. *J. Am. Chem. Soc.* **1984**, *106*, 669.
(18) Cremer, D. *Tetrahedron* **1988**, *44*, 7427.
(19) Exner, K.; Schleyer, P. v. R. *J. Phys. Chem. A* **2001**, *105*, 3407.
(20) Johnston, V. J.; Einstein, F. W. E. B.; Pomeroy, R. K. *J. Am. Chem. Soc.* **1987**, *109*, 8111.
(21) Cr: King, R. B.; Xie, Y.; Schaefer, H. F., III; Richardson, N.; Li, S. *Inorg. Chim. Acta* **2005**, *358*, 1442.
(22) Mn: Xie, Y.; Jang, J. H.; King, R. B.; Schaefer, H. F., III. *Inorg. Chem.* **2003**, *42*, 5219.
(23) Fe, Co, Ni: Schaefer, H. F.; King, R. B. *Pure Appl. Chem.* **2001**, *73*, 1059.
(24) Cu: Li, Q.; Liu, Y.; Xie, Y.; King, R. B.; Schaefer, H. F., III. *Inorg. Chem.* **2001**, *40*, 5842.
(25) Ragaini, F.; Son, M.-S.; Ramage, D. L.; Geoffroy, G. L.; Yap, G. A. P.; Rheingold, A. L. *Organometallics* **1995**, *14*, 387.
(26) Rosa, A.; Baerends, E. J. *New J. Chem.* **1991**, *15*, 815.
(27) Jang, J. H.; Lee, J. G.; Lee, H.; Xie, Y. M.; Schaefer, H. F., III. *J. Phys. Chem. A* **1998**, *102*, 5298.
(28) Braga, D.; Farrugia, L.; Grepioni, F.; Johnson, B. F. G. *J. Organomet. Chem.* **1994**, *464*, C39.
(29) Chevreau, H.; Martinsky, C.; Sevin, A.; Minot, C.; Silvi, B. *New J. Chem.* **2003**, *27*, 1049.
(30) Lo, F. Y.-K.; Longoni, G.; Chini, P.; Lower, L. D.; Dahl, L. F. *J. Am. Chem. Soc.* **1980**, *102*, 7691.
(31) Evans, J. *J. Chem. Soc., Dalton Trans.* **1980**, 1005.
(32) Dunning, T. H. *J. Chem. Phys.* **1970**, *53*, 2823
(33) Huzinaga, S. *J. Chem. Phys.* **1965**, *42*, 1293.
(34) Wachters, A. J. H. *J. Chem. Phys.* **1970**, *52*, 1033.
(35) Hood, D. M.; Pitzer, R. M.; Schaefer, H. F., III. *J. Chem. Phys.* **1979**, *71*, 705.

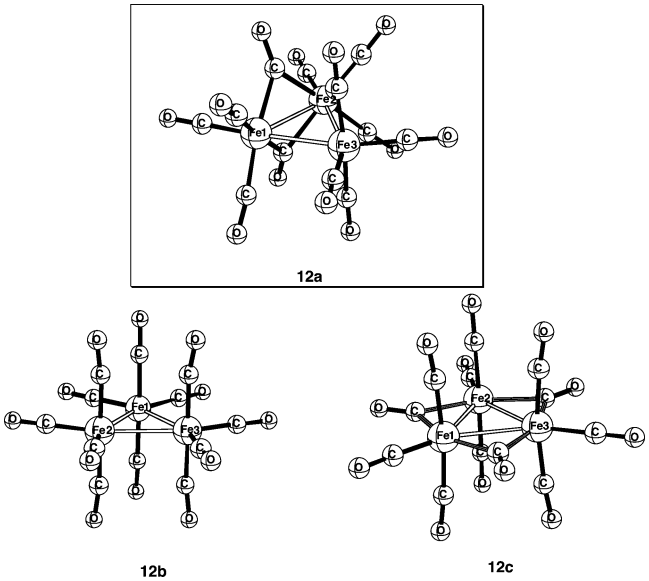

Figure 3. Three $Fe_3(CO)_{12}$ isomers considered in this paper.

Electron correlation effects were included by employing density functional theory (DFT) methods, which have been used as a practical and effective computational tool, especially for organometallic compounds. Two DFT methods were used in this study. The first functional is the hybrid B3LYP method, which incorporates Becke's three-parameter exchange functional (B3) with the Lee, Yang, and Parr (LYP) correlation functional.[36,37] The second approach is the BP86 method, which marries Becke's 1988 exchange functional (B) with Perdew's 1986 correlation functional.[38,39] Both restricted and unrestricted DFT methods were used to explore the stability of the ground state with the same results.

The geometries of all structures are fully optimized with both the DZP B3LYP and DZP BP86 methods. At the same levels the vibrational frequencies are determined by evaluating analytically the second derivatives of the energy with respect to the nuclear coordinates. The corresponding infrared intensities are evaluated analytically as well. All of the computations were carried out with the Gaussian 94 program in which the fine grid (75 302) is the default for evaluating integrals numerically, and the tight (10^{-8} hartree) designation is the default for the energy convergence.[40]

In the search for minima, low-magnitude imaginary vibrational frequencies are suspicious, because the numerical integration procedures used in existing DFT methods have significant limitations. Thus, when one predicts an imaginary vibrational frequency of magnitude less than 100i cm^{-1}, the conclusion should be that there is a minimum of energy identical to or close to that of the stationary point in question.[41] Accordingly, we do not in general follow the imaginary eigenvector in search of another minimum in such cases. All geometries from the computations are depicted in Figures 3−7 with all bond distances reported in angstroms. The global minima for $Fe_3(CO)_n$ (n = 12, 11, 10, 9) are framed in Figures 3, 4, 6, and 7.

3. Results

3.1. $Fe_3(CO)_{12}$. Three structures were optimized for $Fe_3(CO)_{12}$ (Figure 3), namely the experimentally known C_{2v} structure with two bridging CO groups (**12a**), a D_{3h} structure with all terminal CO groups similar to the known structure for $Ru_3(CO)_{12}$ (**12b**), and a second type of D_{3h} structure with three bridging CO groups (**12c**). The C_{2v} dibridged structure **12a** was found to be a genuine minimum without imaginary vibrational frequencies. The D_{3h} unbridged structure **12b** is predicted to lie 6.1 kcal/mol (B3LYP) or 10.3 kcal/mol (BP86) higher in energy than the dibridged structure **12a** in reasonable agreement with the experimental value of ~10 kcal/mol.[7,28] The tribridged structure **12c** lies 8.80 kcal/mol (B3LYP) or 8.72 kcal/mol (BP86) higher in energy than the dibridged structure but has a significant imaginary vibrational frequency of 140i cm^{-1} (B3LYP) or 50i cm^{-1} (BP86). Following the mode represented by this imaginary frequency leads back to the C_{2v} structure **12a**.

Table 1 lists the most important bond lengths and angles for the $Fe_3(CO)_{12}$ structures. For the C_{2v} structure **12a** the CO-bridged Fe−Fe bond length is 2.590 Å (B3LYP) or 2.572 Å (BP86) and the unbridged Fe−Fe bond lengths are 2.736 Å (B3LYP) or 2.713 Å (BP86) as compared with experimental[42] values of 2.56 Å and 2.68 Å, respectively. The two CO bridges are thus found to shorten the Fe−Fe bond in accord with observations on this and other metal carbonyls. The Fe−Fe bonds in the unbridged structure **12b** are found to be 2.767 Å (B3LYP) or 2.741 Å (BP86), similar to the two unbridged Fe−Fe bonds in the C_{2v} structure **12a**. In all three structures, the Fe−C bond lengths are larger for apical CO groups than for equatorial CO groups, whereas the C−O bond lengths are almost the same for both types of CO groups. The C−O bonds in the bridging CO groups of **12a** are increased by about 0.022 Å (B3LYP) and 0.019 Å (BP86) relative to the terminal CO groups. In both D_{3h} isomers **12b** and **12c** the apical C−O bonds are almost parallel to the C_3 axis since ∠CFeC = 179.6°. The angle of the equatorial CO directions ∠CFeC is 104.5° (B3LYP for **12b**) or 102.7° (B3LYP for **12c**). The C_{2v} isomer results in a more efficient angular relaxation. The apical ligands on the unique Fe atom in **12a** are 172.8° (B3LYP) and 172.8° (BP86) slightly bent toward the plane of the iron trimer triangle, whereas the ligands on the other two Fe atoms are in an intermediate position since the ∠CFeC angle is 91.4° (B3LYP) or 97.3° BP86).

3.2. **$Fe_3(CO)_{11}$ and its Radical Anion $Fe_3(CO)_{11}^{\bullet-}$.** In analogy to $Fe_3(CO)_{12}$ discussed above, we tried to optimize tribridged, dibridged, and unbridged structures of $Fe_3(CO)_{11}$. However, we finally obtained only one $Fe_3(CO)_9(\mu_3\text{-}CO)_2$ structure and three $Fe_3(CO)_9(\mu\text{-}CO)_2$ structures (Figure 4 and Table 2).

The lowest energy of these structures is the dibridged structure $Fe_3(CO)_9(\mu_3\text{-}CO)_2$ with nine terminal CO ligands and two CO groups bridging all three iron atoms (**11a**). Structures **11b** (C_s symmetry) and **11c** (C_{2v} symmetry) both have two edges of the Fe_3 triangle bridged by CO ligands and are predicted to lie higher in energy than **11a** by 11.2 kcal/mol (B3LYP) or 17.0 kcal/mol (BP86) for **11b** and 12.5 kcal/mol (B3LYP) or 19.2 kcal/mol (BP86) for **11c**. The relatively long Fe2−Fe3 distance in **11c** of 3.355 Å (B3LYP) or 3.199 Å (BP86) suggests no direct Fe2−Fe3 bond in this structure. However, in **11b** the Fe2−Fe3 distance is only 2.768 Å (B3LYP) or 2.693 Å consistent with an unbridged Fe−Fe single bond.

In constraint of C_{2v} symmetry, we have optimized another dibridged structure, **11d**, similar to **11b**. The resulting structure,

(36) Becke, A. D. *J. Chem. Phys.* **1993**, *98*, 5648.
(37) Lee, C.; Yang, W.; Parr, R. G. *Phys. Rev. B* **1988**, *37*, 785.
(38) Becke, A. D. *Phys. Rev. A* **1988**, *38*, 3098.
(39) Perdew, J. P. *Phys. Rev. B* **1986**, *33*, 8822.
(40) *Gaussian 94*, Revision B.3; Gaussian Inc.: Pittsburgh, PA, 1995 (see Supporting Information for details).
(41) Xie, Y.; Schaefer, H. F., III; King, R. B. *J. Am. Chem. Soc.* **2000**, *122*, 8746.
(42) Cotton, F. A.; Troup, J. M. *J. Chem. Soc., Dalton Trans.* **1974**, 800.

Table 1. Bond Distances (in Å), Bond Angles (in deg), Total Energies (*E* in hartrees), and Relative Energies (Δ*E* in kcal/mol) for the $Fe_3(CO)_{12}$ Isomers

	12a (C_{2v})		**12b** (D_{3h})		**12c** (D_{3h})	
	B3LYP	BP86	B3LYP	BP86	B3LYP	BP86
Fe1−Fe2	2.590	2.572	2.767	2.741	2.720	2.690
Fe1−Fe3, Fe2−Fe3	2.736	2.713				
Fe−C(apical)	1.825	1.815	1.820	1.811	1.833	1.817
C−O(apical)	1.154	1.168	1.155	1.170	1.152	1.167
Fe1−C(equatorial)	1.799	1.784	1.794	1.782	1.777	1.765
C−O(equatorial)	1.153	1.168	1.155	1.169	1.156	1.171
∠CFe1C(equatorial)	101.6	99.2	104.5	102.7	102.7	102.3
Fe−C(bridge)	1.997	1.996			2.005	1.997
C−O(bridge)	1.176	1.187			1.172	1.185
∠FeCFe(bridge)	80.86	80.23			85.4	84.7
−energy	5151.65518	5152.43067	5151.64548	5152.41426	5151.64116	5152.41678
Δ*E*	0	0	6.08	10.30	8.80	8.72
imaginary frequency	No	No	23i	27i, 6i	140i	50i

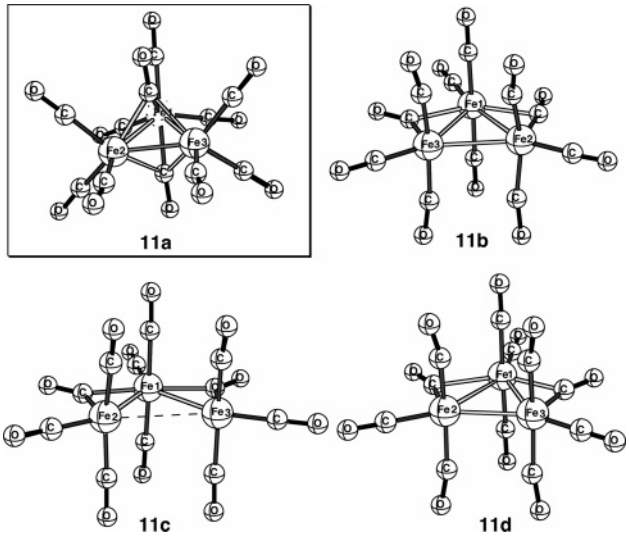

Figure 4. Structures of $Fe_3(CO)_{11}$ isomers.

11d (Table 2 and Figure 4), has a higher energy than **11a** by 22.5 kcal/mol (B3LYP) or 24.4 kcal/mol (BP86), and it is not a minimum since it has large imaginary vibrational frequencies (449i cm^{-1} by B3LYP or 400i cm^{-1} by BP86). Following the mode of the largest imaginary vibrational frequency of **11d** gave **11b** retaining the two bridging CO groups but reducing the symmetry from C_{2v} to C_s.

Although neutral $Fe_3(CO)_{11}$ is not known experimentally, the corresponding radical anion $Fe_3(CO)_{11}^{\bullet-}$ has been isolated and characterized structurally[25] as its tetraphenylphosphonium salt, $[Ph_4P]^+[Fe_3(CO)_{11}]^-$. Optimization of the radical anion $Fe_3(CO)_{11}^{\bullet-}$ structure using the same DFT methods as were used for the other trinuclear iron carbonyls discussed in this paper leads to structure $\mathbf{11}^-$ (Figure 5), with 10 terminal CO groups

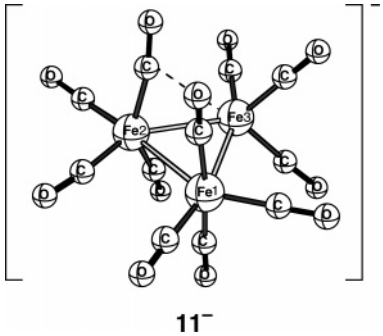

Figure 5. Structure of the $Fe_3(CO)_{11}^{\bullet-}$ radical anion.

and one weakly semibridging CO group in accord with the experimentally determined structure. The computed Fe−C distances to the semibridging CO group in $\mathbf{11}^-$ (dashed line in Figure 5) are 1.802 and 2.684 Å by B32LYP or 1.805 and 2.620 Å by BP86 as compared with the experimentally determined values[25] of 1.885 and 2.488 Å in $[Ph_4P]^+[Fe_3(CO)_{11}]^-$. The computed Fe−Fe distances are 2.570, 2.701, and 2.803 Å by B3LYP or 2.531, 2.744, and 2.744 Å by BP86 as compared with the corresponding experimental values of 2.503, 2.630, and 2.685 Å. Computation and experiment both find the shortest of the three Fe−Fe distances in $Fe_3(CO)_{11}^{\bullet-}$ to be the edge bridged by the semibridging CO group.

3.3. $Fe_3(CO)_{10}$. Structures for $Fe_3(CO)_{10}$ having all terminal CO groups, a single CO bridge, and three CO bridges have been optimized (Figure 6). The unbridged structure **10b** has several imaginary vibrational frequencies, namely 96i, 75i, 40i, and 14i cm^{-1} (B3LYP) or 146i, 110i, 41i, and 23i cm^{-1} (BP86), and thus obviously is not a genuine minimum. The optimized **10a** structure has a CO ligand bridging all three Fe atoms and is the global minimum with only a single imaginary frequency

Table 2. Iron−Iron Bond Distances (in Å), Total Energies (*E*, in hartrees), and Relative Energies (Δ*E*, in kcal/mol) for the Isomers of $Fe_3(CO)_{11}$

	11a (Cs)		**11b** (Cs)		**11c** (C_{2v})		**11d** (C_{2v})	
	B3LYP	BP86	B3LYP	BP86	B3LYP	BP86	B3LYP	BP86
Fe1−Fe2	2.623	2.604	2.865	2.811	2.685	2.647	2.828	2.781
Fe1−Fe3	2.623	2.604	2.839	2.812	2.685	2.647	2.828	2.781
Fe2−Fe3	2.460	2.450	2.768	2.693	3.355	3.199	2.619	2.611
∠213	56	56	58	57	77	74	55	56
−energy	5038.25842	5039.03350	5038.24057	5039.00645	5038.23852	5039.00282	5038.22251	5038.99468
Δ*E*	0	0	11.2	17.0	12.5	19.2	22.5	24.4
imaginary frequencies	23i, 11i	20i, 12i	13i	39i	No	23i	449i, 29i	400i, 50i

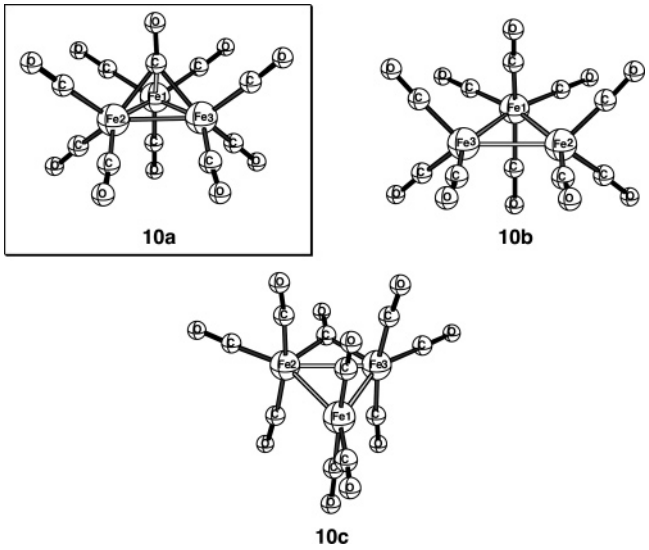

Figure 6. Structures of $Fe_3(CO)_{10}$ isomers.

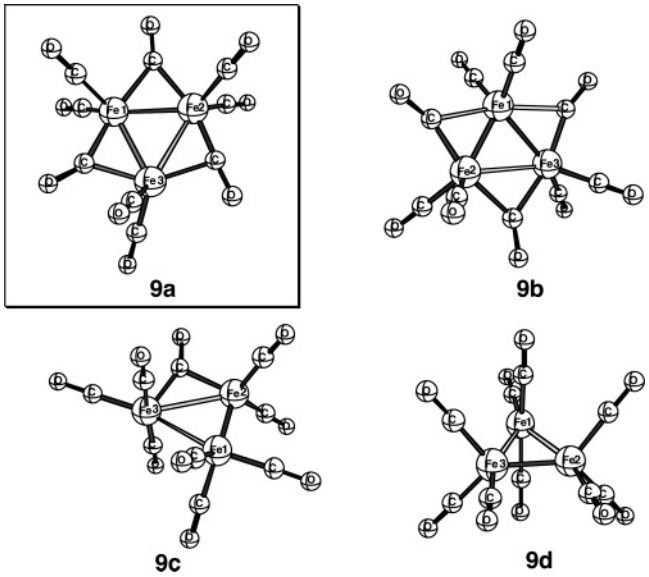

Figure 7. Structures of the $Fe_3(CO)_9$ isomers.

at 17i cm^{-1}. The monobridged **10c** structure has three very small imaginary vibrational frequencies (47i, 33i, 19i cm^{-1} by B3LYP). We interpret these small vibrational frequencies as possibly arising from numerical round off and thus assume that the monobridged structure is a genuine minimum or very close to a genuine minimum.[27] Structure **10c** lies 31.6 kcal/mol (B3LYP) or 32.8 kcal/mol (BP86) above the global minimum **10a**, indicating that in the $Fe_3(CO)_{10}$ system a structure with a CO group bridging all three Fe atoms is energetically more favorable than one bridging only two of the three Fe atoms.

Our lowest-energy $Fe_3(CO)_{10}$ isomer, the C_s symmetry structure **10a**, appears to almost achieve C_{3v} symmetry. Therefore, a constrained optimization in C_{3v} symmetry was carried out. The resulting C_{3v} stationary point lies 2.5 kcal/mol (B3LYP) or 3.9 kcal/mol (BP86) above the C_s symmetry structure **10a**. The three equivalent iron−iron bond distances for the C_{3v} structure are 2.493 Å for B3LYP and 2.494 Å for BP86 (see Table 3).

3.4. $Fe_3(CO)_9$. Two $Fe_3(CO)_9$ structures were initially considered in this research, namely a structure with three bridging CO groups and a structure with only terminal CO groups (Figure 7). The C_s tribridged structure **9a** lies lower in energy than the C_{2v} structure **9b** by 8.1 kcal/mol (B3LYP) or 14.0 kcal/mol (BP86). However, structure **9b** has a large imaginary vibrational frequency, namely 142i cm^{-1}. Following the mode of this imaginary vibrational frequency leads to structure **9a**, which has only a very small imaginary vibrational frequency (25i cm^{-1}) and is thus likely to be a genuine minimum. Structure **9d** is not a genuine minimum since it has an imaginary vibrational frequency above 100i cm^{-1} using either functional. Following the corresponding vibrational mode gives **9c** with a single bridging CO group and eight terminal CO groups. This structure (**9c**), which is 21.6 kcal/mol (B3LYP) or 20.6 kcal/mol (BP86) above the global minimum **9a**, is a genuine minimum or close to a genuine minimum, since it exhibits only two very small imaginary vibrational frequencies (23i and 10i cm^{-1} by B3LYP or 29i and 17i cm^{-1} by BP86). Structure **9c** displays one remarkably short iron−iron distance (Fe1−Fe2) of 2.068 Å (B3LYP) or 2.103 Å (BP86).

Of the $Fe_3(CO)_n$ systems considered here, $Fe_3(CO)_9$ appears to have the lowest-lying triplet electronic state (see Table 4). This is the unbridged $^3A_2'$ state of D_{3h} symmetry, predicted to lie above **9a** by 34.6 kcal/mol (B3LYP) or 52.5 kcal/mol (BP86). The three equivalent iron−iron bond distances are 2.807 Å (B3LYP) or 2.716 Å (BP86). These are clearly Fe−Fe distances corresponding to the unbridged single bonds, corresponding to 16 electrons about each iron atom.

3.5. Vibrational Frequencies. The harmonic vibrational frequencies and their infrared intensities for all the structures have been evaluated by the B3LYP and BP86 methods. Complete reports of the vibrational frequencies and infrared intensities are given in the Supporting Information.

There have been several experimental studies[42,44−46] of the infrared spectrum of $Fe_3(CO)_{12}$, and the assignment of the vibrational frequencies has been reported.[27] The vibrational frequencies for the unsaturated triiron carbonyls $Fe_3(CO)_n$ (n = 9, 10, 11) have not yet been determined experimentally. In

Table 3. Iron−Iron Bond Distances (in Å), Total Energies (E, in hartrees) and Relative Energies (ΔE, in kcal/mol) for the Isomers of $Fe_3(CO)_{10}$

	10a (C_s)		**10b** (C_{2v})		**10c** (C_{2v})	
	B3LYP	BP86	B3LYP	BP86	B3LYP	BP86
Fe1−Fe2	2.468	2.466	2.485	2.442	2.713	2.666
Fe1−Fe3	2.468	2.466	2.485	2.422	2.713	2.666
Fe2−Fe3	2.474	2.474	2.728	2.700	2.680	2.652
∠213	60.1	60.2	66.6	67.1	59.2	59.7
−energy	4924.89175	4925.65587	4924.87382	4925.62044	4924.84140	4925.60356
ΔE	0	0	11.2	22.2	31.6	32.8
imaginary frequencies	17i	52i	96i, 75i, 40i, 14i	146i, 110*i*, 41i, 23i	47i, 33i,19i	55i, 53i, 11i

Table 4. Iron−Iron Bond Distances (in Å), Total Energies (*E*, in hartrees) and Relative Energies (Δ*E*, in kcal/mol) for the Isomers of $Fe_3(CO)_9$

	9a (C_s)		**9b** (C_{2v})		**9c** (C_s)		**9d** (C_{2v})	
	B3LYP	BP86	B3LYP	BP86	B3LYP	BP86	B3LYP	BP86
Fe1−Fe2	2.368	2.343	2.289	2.262	2.068	2.103	2.563	2.452
Fe1−Fe3	2.491	2.473	2.289	2.262	2.716	2.617	2.563	2.452
Fe2−Fe3	2.618	2.601	2.684	2.717	2.769	2.720	2.243	2.344
∠213	65	65	72	74	70	70	52	57
−energy	4811.51448	4812.26830	4811.50152	4812.24606	4811.48006	4812.23547	4811.45426	4812.21099
Δ*E*	0	0	8.13	13.96	21.60	20.61	37.78	35.97
imaginary frequencies	10i	25i	47i	142i	21i	29i, 17i	197i, 38i, 22i	131i, 56i, 32i, 12i

Table 5. Numbers of ν(CO) Frequencies between the Different Ranges of $Fe_3(CO)_n$ (n = 9, 10, 11, 12) Using the BP86 Functional

structure	>1920 cm^{-1}	1700–1920 cm^{-1}	structure	>1920 cm^{-1}	1700–1920 cm^{-1}
12a	10	2	**10a**	9	1
12b	12	0	**10b**	9	1
12c	9	3	**10c**	9	1
11a	9	2	**9a**	6	3
11b	9	2	**9b**	6	3
11c	9	2	**9c**	9	0
11d	9	2	**9d**	9	0

Table 5 the numbers of ν(CO) frequencies in various ranges are listed based on values obtained using the BP86 functional. In the enumeration in Table 5, the ν(CO) frequencies corresponding to doubly degenerate irreducible representations for the structures of D_{3h} symmetry are counted twice in accord with their degeneracies (e.g., structure **12c**).

The numbers of ν(CO) frequencies with values larger than 1920 cm^{-1} in Table 5 are seen to correspond to the numbers of terminal CO groups in the corresponding structures. The lower ν(CO) frequencies in the range 1700 to 1920 cm^{-1} correspond to the bridging CO groups. Within this range the ν(CO) frequencies in the range 1790 to 1920 cm^{-1} correspond to CO groups bridging two Fe atoms (i.e., an edge of the Fe_3 triangle) whereas the ν(CO) frequencies in the range 1730−1785 correspond to CO groups bridging three Fe atoms (e. g., structures **11a** and **10a**).

The radical anion $Fe_3(CO)_{11}^{\bullet-}$ was calculated to exhibit 11 distinct infrared active ν(CO) frequencies in the range 2113−1964 cm^{-1} (B3LYP) or 2032−1895 cm^{-1} (BP86). None of these ν(CO) frequencies appears to correspond to bridging ν(CO) frequencies in accord with the extreme asymmetry of the semibridging CO group. Three of the 11 ν(CO) frequencies for $Fe_3(CO)_{11}^{\bullet-}$ were found to be 10 to 100 times more intense than any of the eight other ν(CO) frequencies. These three intense frequencies in $Fe_3(CO)_{11}^{\bullet-}$ were predicted by the BP86 functional to be 1975, 1967, and 1957 cm^{-1}, which agree well with the most intense frequencies of 1984, 1966, and 1933 cm^{-1} reported for $[Ph_3PNPPh_3]^+[Fe_3(CO)_{11}]^{\bullet-}$ in tetrahydrofuran solution.

4. Discussion

4.1. Unsaturation in Metal Carbonyls. Unsaturated binuclear metal carbonyls can be divided into three general structural types: (1) Structures containing formal metal−metal multiple bonds, (2) structures containing four-electron bridging carbonyl groups and with a lower metal−metal bond order than otherwise required to accommodate the unsaturation, and (3) structures in which one or more metal atoms have less than the favored 18-electron configuration.[21−24] The situation becomes more complicated with unsaturated trinuclear metal carbonyls for the following reasons: (1) The formal metal−metal multiple bonds can be delocalized among the three edges of the M_3 triangle similar to the three formal C═C double bonds in the benzene hexagon. (2) Three-center bonds of various types are possible as indicated by the σ-aromaticity model (Figure 2). (3) A carbonyl group bridging three metal atoms can donate as many as six electrons through one σ bond and two perpendicular π bonds as exemplified by the known[47] structure of $(\eta^5\text{-}C_5H_5)_3Nb_3(CO)_6(\eta^2{-}\mu_3\text{-}CO)$ (Figure 8a).

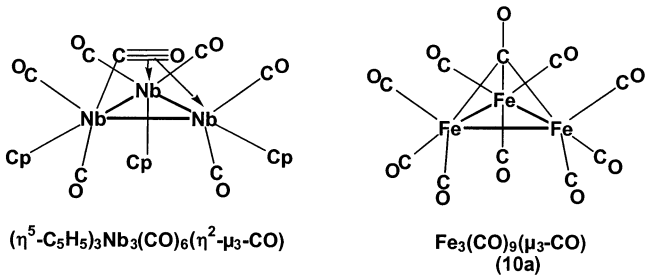

Figure 8. Comparison of the experimentally determined structure of $(\eta^5\text{-}C_5H_5)_3Nb_3(CO)_6(\eta^2\text{-}\mu_3\text{-}CO)$ with the computed structure of $Fe_3(CO)_9(\mu_3\text{-}CO)$ (**10a**) showing the two different types of μ_3-CO groups.

The metal−metal distances may be used as a crude indicator of the sites of metal−metal multiple bonding in unsaturated metal carbonyls. In this connection structural information on $Fe_3(CO)_{12}$ can be used as an indication of the lengths of Fe−Fe single bonds with or without carbonyl bridges. Thus, in isomer **12a** of $Fe_3(CO)_{12}$ the averaged computed values for the two unbridged Fe−Fe bonds are 2.73 Å (B3LYP) or 2.71 Å (BP86), whereas those for the dibridged Fe−Fe bond are 2.59 Å (B3LYP) or 2.57 Å (BP86).

4.2. The $Fe_3(CO)_{11}$ Structures. The lowest-energy isomer for $Fe_3(CO)_{11}$, namely $Fe_3(CO)_9(\mu_3\text{-}CO)_2$ (**11a**) with two μ_3-CO groups bridging the three iron atoms, has significantly unequal Fe−Fe distances in the Fe_3 triangle, in accord with a localized bonding model for the iron−iron bonds. Thus, two of the iron−iron distances in **11a** are 2.623 Å (B3LYP) or 2.604 Å (BP86) corresponding to Fe−Fe single bonds, whereas the third iron−iron distance is only 2.460 Å (B3LYP) or 2.450 Å (BP86), perhaps corresponding to the Fe═Fe double bond required to give all of the iron atoms the favored 18-electron

(43) Bentsen, J. G.; Wrighton, M. S. *J. Am. Chem. Soc.* **1987**, *109*, 4518.
(44) Venter, J. J.; Vannice, M. A. *J. Am. Chem. Soc.* **1987**, *109*, 6204.
(45) Dobos, S.; Nunziante-Cesaro, S.; Maltese, M. *Inorg. Chim. Acta* **1986**, *113*, 167.
(46) Herrmann, W. A.; Biersack, H.; Ziegler, M. L.; Weidenhammer, K.; Siegel, R.; Rehder, D. *J. Am. Chem. Soc.* **1981**, *103*, 1692.
(47) Ishida, S.; Iwamoto, T.; Kabuto, C.; Kira, M. *Nature* **2003**, *421*, 725.

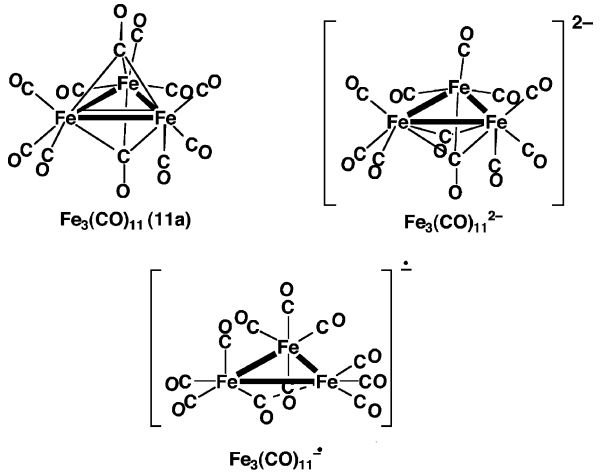

Figure 9. Comparison of the predicted lowest-energy structure of $Fe_3(CO)_{11}$ (**11a**) with the experimentally determined structures of salts of the $Fe_3(CO)_{11}^{2-}$ dianion (b) and the $Fe_3(CO)_{11}^{\bullet-}$ radical anion (c) showing the different arrangements of bridging CO groups.

configuration. This isomer of $Fe_3(CO)_{11}$ (**11a**) could possibly be regarded as a metal carbonyl analogue of cyclopropene in the same sense that $Fe_3(CO)_{12}$ is a metal carbonyl analogue of cyclopropane. However, it must be noted that the iron−iron distance predicted here (2.450Å) is 0.13Å longer than that reported crystallographically for (μ-Bu^{t}C$_2$Bu^t)Fe$_2$(CO)$_6$, a recognized Fe═Fe double bond.[48] Similarly, the experimental Fe═Fe distance[49] in $Cp_2Fe(\mu\text{-}NO)_2FeCp$ is 2.33 Å.

Two distinct higher-energy $Fe_3(CO)_9(\mu\text{-}CO)_2$ isomers are found for $Fe_3(CO)_{11}$ with two edge-bridging CO groups. In **11b** the iron−iron distances are longer than those in the saturated $Fe_3(CO)_{12}$ so that the corresponding Fe−Fe bonds must be single bonds. Thus, one of the iron atoms in **11b** must have a formal 16-electron configuration. Most likely this is the unique iron atom (Fe1) that is bonded to both of the bridging CO groups and thus is seven-coordinate, counting the Fe−Fe bonds. The other $Fe_3(CO)_9(\mu\text{-}CO)_2$ isomer (**11c**) is unusual in having an Fe_3 triangle with one edge too long (3.355 Å by B3LYP or 3.199 Å by BP86) for even an iron−iron single bond. The lengths of the other two edges of the Fe_3 triangle in **11c** (2.685 Å by B3LYP or 2.647 Å by BP86) suggest Fe−Fe single bonds rather than Fe═Fe double bonds so that this isomer cannot be considered as an analogue of a trisilaallene,[48] $R_2Si{=}Si{=}SiR_2$, where the ∠Si═Si═Si angle is significantly bent in contrast to the corresponding angle in allene itself. A detailed bonding scheme in isomer **11c** is highly speculative from currently available information.

It is interesting to compare the structures computed for $Fe_3(CO)_{11}$ (Figure 4) with those found experimentally for the corresponding radical anion[25] $Fe_3(CO)_{11}^{\bullet-}$ and dianion $Fe_3(CO)_{11}^{2-}$ as salts of large cations (Figure 9). Thus, the Ph_4P^+ salt of the radical anion $Fe_3(CO)_{11}^{\bullet-}$ was found by X-ray crystallography to have a structure with 10 terminal CO groups and an eleventh very weakly semibridging CO group with one of its Fe−C distances 2.503 Å. Optimization of the structure of $Fe_3(CO)_{11}^{\bullet-}$ by DFT methods gave a structure (Figure 5) very similar to that found experimentally but with the semibridging CO group bonded somewhat more loosely to the second iron atom (Fe−C distances of 2.684 Å by B3LYP or 2.620 Å by BP86).

The dianion $Fe_3(CO)_{11}^{2-}$ was found by X-ray diffraction on its tetraethylammonium salt[30] to exhibit a structure with one CO group bridging all three iron atoms, similar to bridging by the two μ_3-CO bridges in **11a**. However, the second bridging CO group in $[Et_4N^+]_2[Fe_3(CO)_{11}^{2-}]$ bridges only an edge of the Fe_3 triangle rather than all three Fe atoms as in **11a**. This structure of $Fe_3(CO)_{11}^{2-}$ is thus closer to the lowest-energy structure of $Fe_3(CO)_{11}$ than that of the radical anion $Fe_3(CO)_{11}^{\bullet-}$.

4.3. The $Fe_3(CO)_{10}$ Structures. The global minimum for $Fe_3(CO)_{10}$ (**10a**) has the structure $Fe_3(CO)_9(\mu_3\text{-}CO)$ with a single CO group bridging all three iron atoms in addition to the nine terminal CO groups. All three Fe−Fe distances in the Fe_3 triangle of **10a** are 2.47 Å, suggesting multiple bonding delocalized in the Fe_3 triangle of **10a** rather than localized on a single Fe−Fe edge as in **11a** discussed above. A possible interpretation of the chemical bonding in **10a** includes a 4c-2e Fe_3C bond involving all three Fe atoms in the Fe_3 triangle and the μ_3-CO carbon atom. In this way the lone pair of the unique μ_3-CO group could be simultaneously formally donated to all three iron atoms, thereby compensating for the unsaturation of $Fe_3(CO)_{10}$ without any formal iron−iron multiple bonding. This bonding model for **10a** fits into the σ-aromaticity bonding model in Figure 2b, with the carbon lone pair orbital from the μ_3-CO carbon atom overlapping with the Hückel 3c-2e core bond to convert it into a 4c-2e bond. Superimposition of this 4c-2e bond onto the Möbius 3c-4e perimeter bond in Figure 2b would make an effective iron−iron bond order significantly greater than 1, thereby accounting for iron−iron distances shorter than those expected for single bonds.

Our previous paper on unsaturated binuclear iron carbonyls[41] compared the structure computed for $Fe_2(CO)_7$ with the experimentally determined structure of $(\eta^5\text{-}C_5H_5)_2V_2(CO)_5$. The latter structure is obtained by replacement of one CO group on each iron atom with an η^5-C_5H_5 ring with the necessary adjustment of the metal atoms from iron to vanadium to compensate for the extra three electrons donated by an η^5-C_5H_5 ring relative to a CO group. A similar comparison can be made between the lowest-energy structure **10a** computed for $Fe_3(CO)_{10}$, namely $Fe_3(CO)_9(\mu_3\text{-}CO)$, and the experimentally known[47] $(\eta^5\text{-}C_5H_5)_3Nb_3(CO)_6(\eta^2\text{-}\mu_3\text{-}CO)$ (Figure 8). In $Fe_3(CO)_9(\mu_3\text{-}CO)$ (**10a**) the metals attain the 18-electron configuration by multiple bonding in the Fe_3 triangle with a two-electron donor μ_3-CO group. However, in $(\eta^5\text{-}C_5H_5)_3Nb_3(CO)_6(\eta^2\text{-}\mu_3\text{-}CO)$ the μ_3-CO group is a six-electron donor through a σ bond to one Nb atom and orthogonal π bonds from the C≡O triple bond of the μ_3-CO group to the other two Nb atoms. In this case single bonds in the Nb_3 triangle are sufficient to give all three Nb atoms the favored 18-electron configuration. The difference between $Fe_3(CO)_9(\mu_3\text{-}CO)$ and $(\eta^5\text{-}C_5H_5)_3Nb_3(CO)_6(\eta^2\text{-}\mu_3\text{-}CO)$ probably arises from the greater oxophilicity of the early transition metal Nb relative to that of Fe.

4.4. The $Fe_3(CO)_9$ Structures. The highly unsaturated stoichiometry $Fe_3(CO)_9$ requires a triangle of Fe═Fe double bonds to give each iron atom the favored 18-electron rare gas configuration, assuming the absence of CO groups donating more than two electrons, which is the case for the structures found in this work. However, in the lowest-lying structure **9a**

(48) Cotton, F. A.; Jamerson, J. D.; Stults, B. R. *J. Am. Chem. Soc.* **1976**, *98*, 1774.
(49) Calderón, J. L.; Fontana, S.; Frauendorfer, E.; Day, V. W.; Iske, S. D. A. *J. Organomet. Chem.* **1974**, *64*, C16.

(Figure 6) for $Fe_3(CO)_9$ the Fe_3 triangle does not have the symmetrical distribution of iron−iron distances suggestive of three Fe═Fe double bonds. Instead, in **9a** one of the Fe≡Fe distances is very short (2.368 Å by B3LYP or 2.343 Å by BP86) suggesting a formal triple bond, a second Fe═Fe distance has an intermediate value (2.491 Å by B3LYP or 2.473 Å by BP86) suggesting a formal double bond, and the third Fe−Fe distance (2.618 Å by B3LYP or 2.601 Å by BP86) is in the range for a single bond.

Perhaps helpful in this discussion is Pyykkö's 2005 paper[50] suggesting triple bond covalent radii for the transition metals. In his Figure 1 Pyykkö proposes a value of 1.02 Å for the iron triple bond covalent radius. This in turn suggests a lower bound of 2.04 Å for the Fe≡Fe triple bond. Such a lower bound is consistent with the experimental Fe≡Fe bond distance (2.18 Å) reported[51] for (η^4-Ph_4C_4)Fe(μ-CO)$_3$Fe(η^4-C_4Ph_4). In this context it would appear that the present 2.343 Å distance in **9a** is too long to be a true triple bond. Note, however, the experimental structure[51] is triply bridged, yielding an Fe≡Fe distance significantly shorter than would be expected from the singly bridged structure **9a**.

A clearer interpretation is possible for the other true $Fe_3(CO)_9$ minimum **9c**, which lies 21.6 kcal/mol (B3LYP) or 20.6 kcal/mol (BP86) above the global minimum **9a**. Structure **9c** has one very short iron−iron bond (2.068 Å by B3LYP or 2.103 Å by BP86) and two Fe−Fe single bonds (2.769 and 2.716 Å by B3LYP or 2.720 and 2.617 Å by BP86). The short iron−iron distance would be compatible with Pyykkö's definition of the Fe≡Fe triple bond. However, since the only known Fe≡Fe triple bond has an iron−iron separation of 2.18 Å (previous paragraph), it seems more reasonable to identify **9c** with a quadruple bond. The difference in the Fe−Fe distances for the two formal single bonds in **9c** arises from the fact that one is bridged by a CO group and the other is unbridged.

4.5. Reciprocal Diagonal Compliance Matrix Elements. The variation in the iron−iron bond orders in the global minimum of $Fe_3(CO)_9$ (**9a**) is consistent with our examination of the compliance matrix[52−54] of the iron−iron bonds in its Fe_3 triangle, obtained using a method similar to that recently used for binuclear iron and cobalt carbonyls.[55] Thus, the reciprocal diagonal compliance matrix elements $1/C_{ii}$ in aJ/Å^2 for the three iron−iron bonds in the $Fe_3(CO)_9$ global minimum **9a** (Figure 7), all of which are bridged by single CO groups, were found to be 1.04, 0.96, and 0.83 aJ/Å for the Fe1−Fe2, Fe2−Fe3, and Fe3−Fe1 edges, respectively, corresponding to an Fe≡Fe triple bond, an Fe═Fe double bond, and an Fe−Fe single bond on the basis of the iron−iron distances as discussed above. For comparison, the $1/C_{ii}$ values found[55] for binuclear cobalt carbonyls with a single bridging CO group are 1.01 aJ/Å for an isomer of $Co_2(CO)_6(\mu$-CO) with a formal Co═Co double bond and 1.40 aJ/Å for an isomer of $Co_2(CO)_4(\mu$-CO) with a formal Co^{-4}−Co quadruple bond.

Since one of the predicted iron−iron distances for structure **9c** is so short, 2.068 Å or 2.103 Å, it might be considered (following the 18-electron rule) an Fe^{-4}−Fe quadruple bond. Such a suggestion is consistent with the value 1.83 aJ/Å^2 predicted for $1/C_{ii}$ for this iron−iron bond. The two iron−iron distances in **9a** assigned as single bonds have much smaller values of $1/C_{ii}$, namely 0.59 (the unbridged bond) and 0.82 aJ/Å (the bridged bond). In this and other cases, we find bridging carbonyls to increase the values of $1/C_{ii}$ for metal−metal bonds.

It must be noted that the compliance matrices for these metal−metal bonds cannot be directly compared with those for standard hydrocarbon compounds. Thus, for acetylene, ethylene, and ethane the predicted $1/C_{ii}$ values (at the same level of theory) are 15.8, 9.0, and 4.0 aJ/Å^2, respectively.

4.6 Bond Indices. Helpful though the vibrational frequencies and compliance matrices may be, it can be challenging (see above) to separate out the effects of bridging carbonyls from the derivation of realistic bond orders. To cite a dramatic example, $1/C_{ii}$ for the Fe−Fe linkage in $Fe_2(CO)_9$ is 2.05 aJ/Å, the largest value predicted for all the Fe−Fe bonds considered here. Yet, there is growing agreement[56−62] that the Fe−Fe bond in $Fe_2(CO)_9$ has bond order less than 1. Thus, the three bridging carbonyls are obscuring the weak Fe−Fe bond. The advantage of frequencies and compliance matrices is that, at least in principle, these quantities may be obtained directly from experiment.

All attempts to analyze molecular electron densities in terms of bond orders are necessarily, at least to some degree, arbitrary. Again, in principle, the electron density can be obtained from experiment. The challenge is to deduce bond orders from the observed electron density.

Here we have used the Wiberg Bond Index (WBI)[63,64] in an attempt to further experimentally understand the bonding in these iron trimer carbonyl systems. We note before starting that all transition metal-transition metal WBIs are much smaller than for carbon−carbon bonds. This is perhaps best seen for structure **12b**, analogous to the experimentally known ground-state structures of $Ru_3(CO)_{12}$ and $Os_3(CO)_{12}$. With no bridging carbonyls, the $Fe_3(CO)_{12}$ structure is essentially "forced" to have three Fe−Fe single bonds. If structure **12b** does not have three single bonds, then the concept of chemical bonding in organotransition metal chemistry is less than meaningful. The WBIs for the three Fe−Fe bonds **12b** are 0.18. Although far below the value of 1.0, we take this value to correspond to the standard Fe−Fe single bond.

This standard Fe−Fe WBI may be compared with the analogous value for the controversial $Fe_2(CO)_9$ system, which Coppens and others[56−62] have concluded not to have an Fe−Fe single bond. For $Fe_2(CO)_9$, the Fe−Fe WBI is 0.11. On this basis $Fe_2(CO)_9$ might be concluded to have a bond order somewhat greater than 1/2 . This analysis is consistent with that deduced for **12a**, the experimentally known ground state for $Fe_3(CO)_{12}$. There the two unbridged Fe−Fe single bonds show a WBI of 0.18, while the dibridged Fe−Fe bond has WBI

(50) Pyykkö, P.; Riedel, S.; Patzschke, M. *Chem. Eur. J.* **2005**, *11*, 3511.
(51) Murahashi, S.-I.; Mizoguchi, T.; Hosokawa, T.; Montani, I.; Kai, Y.; Kohara, N.; Kasai, N. *Chem. Commun.* **1974**, 563.
(52) Decius, J. C. *J. Chem. Phys.* **1962**, *38*, 241.
(53) Jones, L. H.; Swanson, B. I. *Acc. Chem. Res.* **1976**, *9*, 128.
(54) Grunenbeg, J.; Goldberg, N. *J. Am. Chem. Soc.* **2000**, *122*, 6045.
(55) Xie, Y.; Schaefer, H. F., III. *Z. Phys. Chem.* **2003**, *217*, 189.
(56) Summerville, R. H.; Hoffmann, R. *J. Am. Chem. Soc.* **1979**, *79*, 1501.
(57) Heijser, W.; Baerends, E. J.; Ros, P. *Faraday Symp. Chem. Soc.* **1980**, *14*, 211.
(58) Bauschlicher, C. W. *J. Chem. Phys.* **1986**, *84*, 872.
(59) Rosa, A.; Baerends, E. J. *New J. Chem.* **1991**, *15*, 815.
(60) Bo, C.; Sarasa, J.-P.; Poblet, J.-M. *J. Phys. Chem.* **1993**, *97*, 6362.
(61) Reinhold, J.; Hunstock, E. *New J. Chem.* **1994**, *18*, 465.
(62) Koritsanszky, T. S.; Coppens, P. *Chem. Rev.* **2001**, *101*, 1583.
(63) Wiberg, K. B. *Tetrahedron* **1968**, *24*, 1083.
(64) Weinboid, F.; Landis, C. R. *Valency and Bonding: A Natural Bond Order Donor-Acceptor Perspective*; Cambridge University Press: New York, 2005.

= 0.09. Interestingly the shorter (dibridged) Fe−Fe distance (2.572 Å) has the smaller WBI compared to those (2.713 Å) for the two unbridged Fe−Fe single bonds. Again, the absence of a substantial Fe−Fe bond order is concealed by the short Fe−Fe distance arising from bridging carbonyls.

The D_{3h} structure **12c** may be subjected to the same analysis. With three equivalent dibridging carbonyls, the iron−iron WBIs are all 0.10. Thus, structure **12c** is held together primarily by the bridging carbonyls, with iron−iron bond orders of about 1/2.

Moving to the unsaturated iron trimer carbonyls, the WBI for lowest-energy isomer **11a** are 0.15 (two of these) and 0.25. These correspond to the longer (2.604 Å) and shorter (2.450 Å) iron−iron bonds, which may roughly be described as single and weak double bonds (perhaps bond order 3/2), respectively. For structure **11b**, the WBIs are 0.20 (2.812 Å Fe−Fe distance), 0.16 (2.811 Å), and 0.18 (2.693 Å). All three Fe−Fe bonds are apparently single bonds. Structure **11d** (C_{2v} symmetry) has iron−iron distances and WBI as follows: 2.781 Å (0.16), 2.781 Å (0.16) and 2.611 Å (0.26). The unbridged iron−iron bond (2.611 Å) is clearly the strongest and we might estimate the bond order as 3/2. Thus we are missing about half a bond to satisfy the 18-electron rule.

For $Fe_3(CO)_{10}$ to fulfill the 18-electron rule, one needs two double bonds or one triple iron≡iron bond. The lowest-energy structure for $Fe_3(CO)_{10}$ is **10a**, not too far from C_{3v} symmetry. In fact, all three WBIs are 0.24, suggesting bond orders something like 4/3. Here we fall short of the 18-electron rule by about one bond. For the C_{2v} structure **10b**, we have iron−iron distances and WBIs of 2.442 Å (0.23), 2.442 Å (0.23), and 2.700 Å (0.17). The latter bond seems a conventional Fe−Fe single bond, while the two equivalent bonds might be assigned bond orders of 4/3.

The most interesting predicted WBI is for the $Fe_3(CO)_9$ structure **9c**, which contains the very short (2.068 or 2.103 Å) unbridged iron−iron bond distance, possibly an $Fe^{\overline{4}}$—Fe quadruple bond. In fact the WBI supports this interpretation! The WBI value for this ultrashort iron−iron distance is 0.78, slightly more than 4 times our standard value (0.18) for an unbridged Fe−Fe single bonds. The two Fe−Fe single bonds in this structure (**9c**) have the conventional WBI values 0.20 (unbridged) and 0.21 (bridged). This analysis provides significant support for the hypothesis that structure **9c** incorporates an $iron^{\overline{4}}$—iron quadruple bond.

Acknowledgment. We are grateful to the National Science Foundation for support of this work under Grant CHE-045144. H.W. thanks the China Scholarship Council for financial support (CSC No. 2003851025) and National Natural Science Foundation of China (Grant No. 10276028).

Supporting Information Available: Complete tables of harmonic vibrational frequencies for $Fe_3(CO)_n$ (n = 12, 11, 10, 9) and $Fe_3(CO)_{11}^{\bullet-}$ (Tables S1−S15); structures with complete bond distances for $Fe_3(CO)_n$ (n = 12, 11, 10, 9) and $Fe_3(CO)_{11}^{\bullet-}$ (Figures S1− S5); complete ref 40. This material is available free of charge via the Internet at http://pubs.acs.org.

JA055223+